Theoretical Study of Modes of Adsorption of Water Dimer on H-ZSM-5 and H-Faujasite Zeolites

Siriporn Jungsuttiwong,[†,‡] Jumras Limtrakul,*[,‡] and Thanh N. Truong*[,†]

Henry Eyring Center for Theoretical Chemistry, Chemistry Department, University of Utah, 315 S 1400 E, Room 2020, Salt Lake City, Utah 84112, and Laboratory for computational and applied chemistry, Chemistry Department, Kasetsart University, Bangkok 10900, Thailand

Received: November 1, 2004; In Final Form: April 26, 2005

Modes of adsorption of water dimer on H-ZSM-5 and H-Faujasite (H-FAU) zeolites have been investigated by a quantum embedded cluster approach, using the hybrid B3LYP density functional theory. The results indicate that there are two possible adsorption pathways, namely the stepwise process where only one water binds strongly to the $(-O)_3$-Al-O(H) tetrahedral unit while the other weakly binds to the zeolite framework and the concerted process where both water molecules form a large ring of hydrogen-bonding network with the Brønsted proton and an oxygen framework. With inclusion of the effects of the Madelung potential from the extended zeolite framework, for adsorption on H-ZSM-5 zeolite, both the neutral and ion-pair complexes exist with adsorption energies of −15.13 and −14.73 kcal/mol, respectively. For adsorption on the H-FAU, only the ion-pair complex exists with the adsorption energy of −14.63 kcal/mol. Our results indicate that adsorption properties depend not only on the acidity of the Brønsted acidic site but also on the topology of the zeolite framework, such as on the spatial confinement effects which lead to very different adsorption structures for the ion-pair complexes in H-ZSM-5 and H-FAU, even though their adsorption energies are quite similar. Our calculated vibrational spectra for these ion-pair complexes support previous experimental IR interpretations.

Introduction

Zeolite Brønsted acid sites have been known to catalyze many industrially important processes such as hydrocarbon conversions and production of fine chemicals. Protonation of substrate molecules by Brønsted protons has been suggested, and in fact is well-accepted as the initial step of these processes. For this reason, understanding whether substrate molecules are protonated upon adsorption on a Brønsted acid site is of great fundamental and technological importance. However, adsorption of a weak base such as water presents a challenge for experimental identification of its mode of adsorption. Two possible structures have been suggested when H_2O is adsorbed at the Brønsted acid site: a hydrogen-bonded or a protonated complex. The preferred equilibrium structure has been a heavily debated issue. There are challenges in both experimental and theoretical investigations making the task of resolving this controversial issue more difficult.[1−12]

Adsorption of an isolated water molecule on a Brønsted acidic site has been well-accepted and confirmed to form a neutral hydrogen-bonded complex. The remaining controversial issue is the number of water molecules needed to stabilize the protonated species. In previous experimental results, mostly obtained by IR spectroscopy, Jentys et al.[4] reported that protonation was observed by further adsorption of H_2O to the 1:1 hydrogen-bonded structure on H-ZSM-5 to form dimeric $H_5O_2^+$ and polymeric $H_5O_2^+n(H_2O)_n$ species. In another IR study, Kondo et al.[13] also indicated that the IR spectra of the dimeric $H_5O_2^+$ species were clearly observed. In yet a different IR study, Zecchina and co-workers suggested that $H^+(H_2O)_n$ ionic species are formed at a high dosage of two or more water molecules per site.[14] However, Jobic et al.[15,16] using the Inelastic Neutron Scattering technique to also study adsorption of water at different concentrations in H-ZSM-5 did not observe the formation of hydroxonium ions. These studies pointed out the difficulty in interpreting the experimental spectra, particularly at higher loading levels, due to the possibility of interferences from the channel walls, the coexistence of both the hydrogen-bonded and protonated species in equilibrium condition, and the multiple possible structures of a species for a given cluster size.

Theoretical results obtained by Zygmunt et al.[17] using a 5T (five tetrahedral sites) cluster model found that the neutral complex is more stable than the ion-pair structure by 2.9 kcal/mol; this finding is consistent with those of Gale et al.,[18] Bell et al.,[19] and Limtrakul et al.[12,20] On the other hand, the results obtained by Krossner et al.[21] using exactly the same 5T model as Zygmunt at a different level of theory (BP for the former versus the B3LYP for the latter) found the ion-pair complex is more stable by about 3.6 kcal/mol. These studies agree that both neutral hydrogen bonded and ion-pair complexes exist. However, the predicted adsorption structures and their relative stabilities vary greatly. The differences could be due to several different sources such as differences in the level of theory and the physical model of the zeolite active site used. It is interesting to point out that the effects of the Madelung potential from the extended zeolite structure were not included in any of these studies. Such effects have been known to stabilize the ion-pair complexes[22,23] and thus, one would expect they play a significant

* Address correspondence to these authors. E-mail: truong@chemistry.utah.edu (Thanh N. Truong) and fscijrl@ku.ac.th (Jumras Limtrakul).

† University of Utah.

‡ Kasetsart University.

10.1021/jp045021k CCC: $30.25
Published on Web 06/21/2005

role in determining the adsorption structures of water dimer on zeolites. Furthermore, the most recent theoretical study done by Zygmunt et al.[17] concluded that the 3T and 5T cluster models used so far are not adequate for studying adsorption of water dimer due to the possibility for water dimer to interact with the "capped" hydrogen atoms.

The importance of a fundamental understanding of factors that can affect the mode of adsorption, the lack of conclusive evidence in experimental data, and the shortcomings of previous theoretical studies have motivated us to perform a more systematic theoretical investigation on the adsorption of water dimer on zeolites. In particular, in this study, in addition to taking into account the effects of electron correlation, of large basis set, and of the zero-point energy motions, the effects of the long-range Madelung potential from the extended zeolite framework are also included in the determinations of both adsorption structures and the relative stability of the two forms of adsorption complexes by using an embedded cluster model. With such a model, it allows theoretical investigation on the effects of different zeolite structures on the adsorption properties. Particularly, we considered the adsorption on H-ZSM-5 and H-FAU zeolites. ZSM-5 has the channel cross section of 5.6 Å, whereas FAU has a 7.4 Å cross section. How the differences in the ZSM-5 and FAU zeolite structures affect the adsorption mode is a question that has not been addressed previously. Our results also indicated that formation of the water dimer complex adsorbed on a Brønsted acid site can originate from two separate pathways, which yield two different adsorption structures. In one pathway, the dimer adsorption complex is formed by adsorbing one water molecule at a time on the adsorption site in a stepwise process. In this case, the first water molecule binds to the O_3-Al-O(H) tetrahedral unit more strongly while the second water molecule binds to the first water molecule and the zeolite framework. In the other pathway, the dimer adsorption complex is formed by adsorption of water dimer on the adsorption site in a concerted process. In this case, both water molecules form a larger ring with the Brønsted acid site and a nearby oxygen of the zeolite framework. Addressing the question of how these pathways manifest in the mode of adsorption of water dimer on zeolite is also part of this study. Furthermore, comparisons between the calculated and experimental IR spectra allow verifications on the experimental suggested fingerprints for the ion-pair complex species.

Computational Details

In this study, to avoid unphysical interactions between adsorbates and capped hydrogen atoms, quantum clusters consisting of seven tetrahedrally coordinated atoms (Si, Al) from the crystal structures[24] were selected to represent the Brønsted acidic sites of these zeolites which are parts of the 12-membered ring of FAU or the 10-membered ring of ZSM-5 zeolites. These rings are at the intersections of the channels and are accessible to the adsorbates. Hydrogen atoms were used to cap the dangling bonds. These capped hydrogen atoms are located along the direction of corresponding Si−O bonds. The resulting 7T clusters, $Si_6AlO_{10}H_{16}$, have a total of 34 atoms. For ZSM-5 zeolite, the T12 site was selected to represent the active site because it was found to be among the most stable sites for Al substitution,[25,26] and this site provides sufficient space and can be accessed easily by small adsorbates. Most previous theoretical works have also chosen the T12 site as the Al substitution site for ZSM-5 zeolite. For FAU, all of the T sites (Al or Si tetrahedral sites) are equivalent by symmetry.

In the embedded cluster models, the 7T clusters are embedded in an array of point charges that represent the static Madelung potential due to atoms outside the quantum cluster. Our previous study[27] indicated that the embedded 7T cluster model would be sufficient for studying adsorption of molecules with binding energies less than 40 kcal/mol; that is the case here as discussed below. Using the Surface Charge Representation of External Embedded Potential (SCREEP) method developed by Stefanovich and Truong,[28] the Madelung potential owing to the extended zeolite structure is represented by two sets of point charges. For atoms located within the unit cell of the quantum cluster, they are represented explicitly by point charges located at the lattice positions. The magnitudes of these point charges are taken from periodic population analyses of zeolite systems. To minimize the interaction that occurs between the quantum mechanical terminating hydrogen atoms and the neighboring point charges, the first layer of explicit point charges nearest to the quantum cluster were removed and these charges are redistributed among the second shell (the next layer) explicit point charges. Specifically, the charges on the second shell are fitted to reproduce the original potential in the active center due to both the first and second shells. The Madelung potential from the remaining charges of an infinite lattice is represented by a set of surface charges that were derived from the SCREEP method (see Figure 1). More details on this method can be found elsewhere.[29,30] For H-FAU (see Figure 2), the total Madelung potential is represented by 441 explicit charges and 1311 surface charges, whereas for the H-ZSM-5 (see Figure 3), 564 explicit charges and 978 surface charges are employed. Note that pure SiO_2 FAU and ZSM-5 crystal structures were used in calculating the static Madelung potential therefore Si/Al ratio effects are not included in this study.

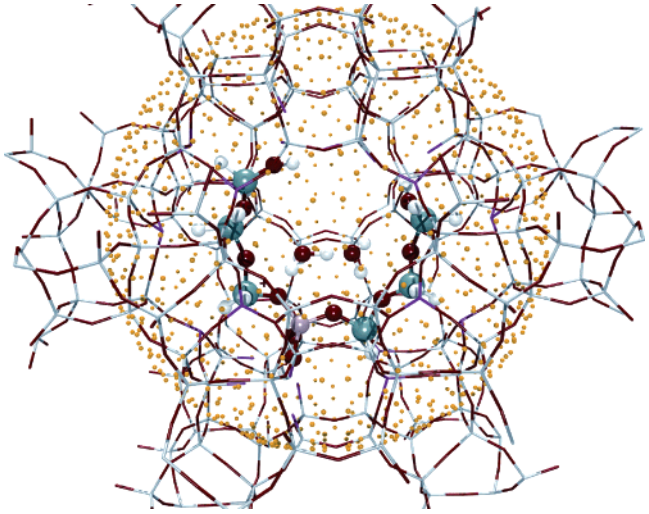

Figure 1. Illustration of the SCREEP embedded cluster model. The Madelung potential from periodic framework is represented by two sets of point charges, i.e., surface charges and explicit charges.

The hybrid B3LYP density functional theory was used in this study. In all structural determinations, geometries of the 3T cluster surrounding the active site (Si-O1H-Al-O2-Si) and of the water dimer are fully optimized while the remaining part of the 7T quantum cluster is fixed in their lattice positions. For these calculations, a mixed basis set was used. In particular, the 6-31G(d,p) basis set was used for all atoms in the small 3T cluster containing the active center and the water dimer mentioned above, whereas the 3-21G basis set was used for the remaining atoms of the larger 7T cluster. Single-point B3LYP calculations at a larger basis set were also done. Similarly, a mixed-basis set was used in this case where the larger 6-311+G(3df,2p) basis set was used for the smaller 3T

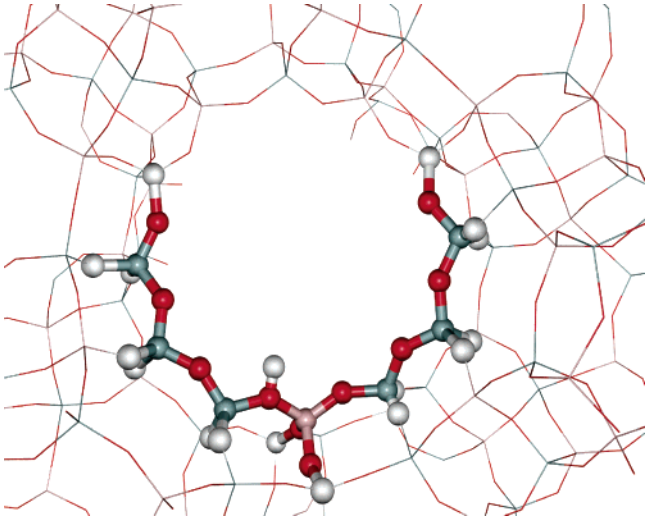

Figure 2. The 7T embedded cluster model for H-Faujasite.

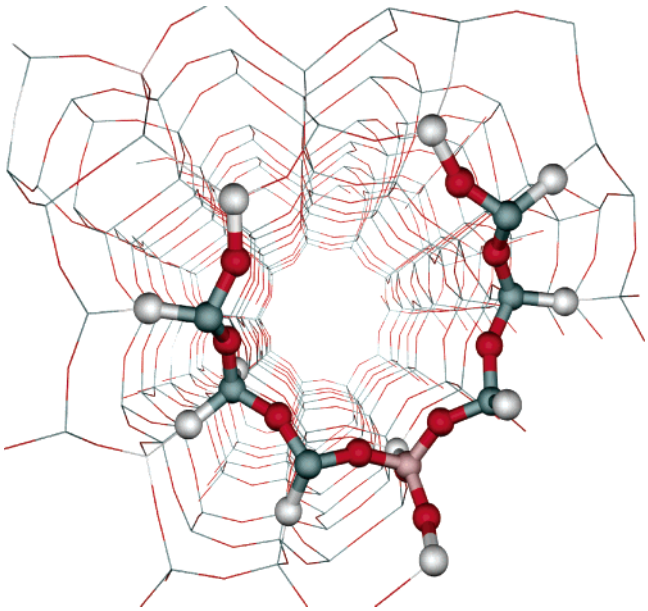

Figure 3. The 7T embedded cluster model for H-ZSM-5.

cluster and the water dimer instead of the 6-31G(d,p) one. Note that the 6-311+G(3df,2p) basis set used in the G2 theory for the effects of large basis set was also used previously by Zygmunt et al. for studying the same system, but with a smaller cluster. Normal-mode analyses using the embedded cluster model were also carried out to verify the nature of the adsorbed complexes and their IR spectra. All calculations were done with the GAUSSIAN 98 program.[31]

Results

In this study, we focus only on the possible modes of adsorption of water dimer on two different zeolites, namely FAU and ZSM-5. Previous theoretical studies have reported two different ways for calculating the "adsorption energy" of water dimer, specifically:

$$\Delta E_{ads} = E(\text{complex}) - E(\text{free zeolite}) - E(\text{water})_n \quad (1)$$

$$\Delta E_{ads} = E(\text{complex}) - E(\text{free zeolite}) - nE(\text{water}) \quad (2)$$

In eq 1,[20] the adsorption energy is referenced to the energy of the infinite separation of water dimer and zeolite, whereas in eq 2[21] it is referenced to the energy of infinite separation of zeolite and two isolated water molecules. The latter is closer to the definition of the formation energy of water dimer on zeolite. In this study, we used eq 1 for calculating adsorption energies. To compare with the results that came from the use of eq 2, the binding energy of water dimer, $E_b(H_2O)_2 = E(\text{water})_n - nE(\text{water})$, should be added. The binding energy of water dimer calculated at the B3LYP/6-311++G(3df,2p)//B3LYP/6-31G(d,p) level is 3.23 kcal/mol.

There are two possible modes of adsorption of water dimer on zeolites, namely the neutral and ion-pair complexes, denoted as NC and IP complexes, respectively, in this study. The NC complex is where water dimer is stabilized by forming hydrogen bonds with the Brønsted acid site and the framework oxygen atom. In the IP complex, the Brønsted acidic proton transferred to the water dimer to form an $H_5O_2^+$ hydronium ion, which is stabilized by forming strong hydrogen bonds with the deprotonated zeolite framework. Both such complexes can coexist and be stabilized by the zeolite framework. If so, there would be a transition state connecting these two stable structures. Zygmunt et al.[17] found that such a transition state has a rather low barrier and thus one can expect that these two complexes, if both existed, would be in rapid thermal equilibrium. For this reason, in this study, we only focus on the stable adsorption structures. Our results indicate that there are two possible adsorption pathways for each adsorption mode. One pathway leads to the adsorption structure that has one water molecule of the dimer forming two strong hydrogen bonds to the $(-O)_3$-Al-OH tetrahedral unit to yield a 6-membered ring structure similar to that of the adsorption of a single water molecule, while the other water molecule does not have any direct interaction with the $(-O)_3$-Al-OH tetrahedral unit, but binds to the other water and the zeolite framework. This water dimer adsorption complex can be thought to be formed by a stepwise adsorption process, i.e., adsorption of a single water molecule at a time on the adsorption site. The other pathway yields the adsorption structure that has both water molecules forming a larger ring where one of the two water molecules makes only one hydrogen bond to the acidic proton while the other water molecule forms a hydrogen bond with the oxygen atom of the nearby tetrahedral unit of the cross section. This complex can be thought to be formed by a concerted adsorption process of water dimer on the adsorption site. These adsorption structures are somewhat different from those reported by Krossner and Sauer[21] and Zygmunt et al.,[17] where both water molecules form hydrogen bonds with only oxygen atoms of the $(-O)_3$-Al-O(H) tetrahedral unit. This is because the cluster model used in these studies has only these four oxygen atoms of the $(-O)_3$-Al-O(H) tetrahedral unit for forming hydrogen bonds with the water dimer, thus it would not be able to predict the adsorbed structures found here. In addition, in the actual ZSM-5 and FAU zeolite framework, two of the oxygen atoms of the $(-O)_3$-Al-O(H) tetrahedral unit that are not on the zeolite cross section (the two OH groups in Figures 2 and 3) have their lone pairs pointing away and thus would not make a strong hydrogen bond with the water dimer. Such adsorption structure may still exist at a weaker binding energy; however, accurate determination of its structure would require larger quantum clusters than those used in this study and thus is beyond our current computing capability. Note that under experimental conditions, conversion between these possible adsorption complexes is possible due to thermal fluctuations. Further discussion on these structures is given below. It is important to point out that since we employed both the cluster and embedded cluster models and

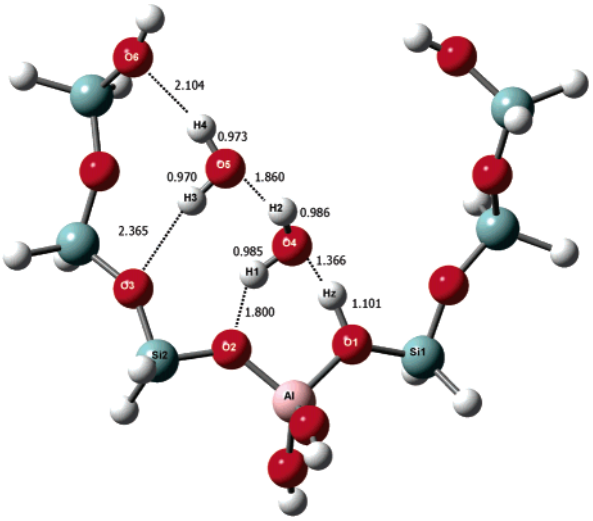

Figure 4. Structure of the neutral complex of the $(H_2O)_2$/H-ZSM-5 system optimized at the B3LYP/6-31G(d,p) level, using the cluster model (bond distances are in Å).

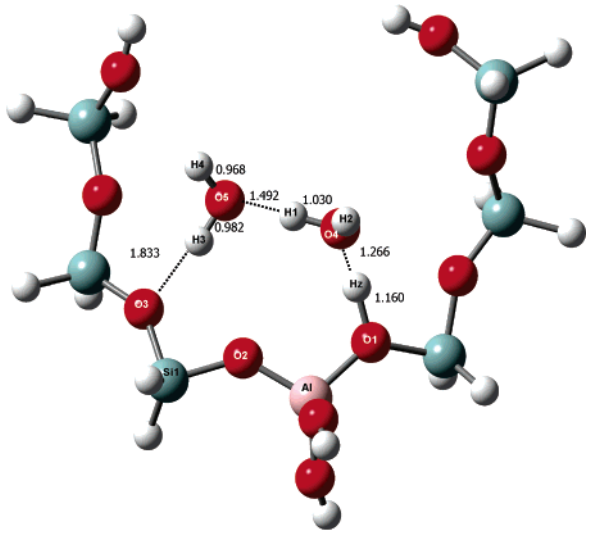

Figure 5. Structure of the neutral complex of the $(H_2O)_2$/H-ZSM-5 system optimized at the B3LYP/6-31G(d,p) level, using the embedded cluster model (bond distances are in Å).

the latter model is more accurate, thus, results from the cluster model are only used to illustrate the importance of the Madelung field effects. To make comparisons with experimental observations, results from the embedded cluster model are used.

Adsorption of Water Dimer on H-ZSM-5. Optimized adsorption structures of water dimer on H-ZSM-5 are shown in Figure 4, using the cluster model, and Figures 5 and 6, using the embedded cluster model. Selected bond distances are also given in the figures. Additional selected optimized geometrical parameters and calculated adsorption energies are listed in Tables 1 and 2, respectively.

To include the effect of the large basis set, our calculated adsorption energies are carried out at B3LYP/6-311+G(3df,-2p)//B3LYP/6-31G(d,p). The cluster model predicts adsorption of water dimer on H-ZSM-5 in only the NC form with the zero-point energy (ZPE) corrected adsorption energy of −14.57 kcal/mol, whereas the embedded cluster model predicts both forms, NC and IP, existing in nearly equal population with the ZPE-corrected adsorption energies of −15.13 and −14.73 kcal/mol, respectively. Since results from previous cluster models do not include the effects of the zeolite crystal framework, they can

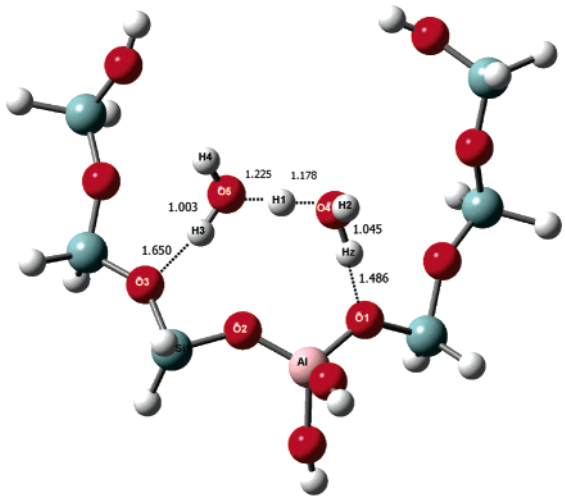

Figure 6. Structure of the ion-pair complex of the $(H_2O)_2$/H-ZSM-5 system optimized at the B3LYP/6-31G(d,p) level, using the embedded cluster model (bond distances are in Å).

TABLE 1: Selected Optimized Geometrical Parameters (bond lengths in Å and angles in deg) and Adsorption Energies (kcal/mol per water molecule) for Water Dimer Adsorption on ZSM-5, Using Both the Cluster and Embedded Cluster Models

cluster		embedded cluster		
	NC (Figure 4)		NC (Figure 5)	IP (Figure 6)
O_1-Hz	1.10	O_1-Hz	1.16	1.49
O_4- - -Hz	1.37	O_4- - -Hz	1.27	1.04
O_2- - -H_1	1.80	O_4-H_1	1.03	1.18
O_4-H_1	0.98	O_5- - -H_1	1.49	1.22
O_4-H_2	0.99	O_5-H_3	0.98	1.00
O_5- - -H_2	1.86	O_3- - -H_3	1.83	1.65
O_5-H_3	0.97	O_3-Si_1	1.68	1.70
O_3- - -H_3	2.36	Si_1-O_2	1.65	1.65
O_6- - -H_4	2.10	O_2-Al	1.65	1.65
O_1-Al	1.78	O_1-Al	1.70	1.67
O_2-Al	1.70	$\angle O_1AlO_2$	106.4	108.6
$\angle O_1AlO_2$	93.7	$\angle AlO_2Si_1$	132.5	132.8
$\angle H_1O_2Al$	113.7	$\angle O_2Si_1O_3$	90.2	89.3
$\angle O_4H_1O_2$	138.9	$\angle Si_1O_3H_3$	111.0	107.1
$\angle HzO_4H_1$	91.0	$\angle O_3H_3O_5$	167.4	165.8
$\angle O_1HzO_4$	162.3	$\angle H_3O_5H_1$	111.0	114.6
$\angle O_4H_2O_5$	150.8	$\angle O_5H_1O_4$	177.9	177.4
$\angle H_3O_5H_2$	93.8	$\angle H_1O_4Hz$	115.5	112.3
$\angle O_3H_3O_5$	158.8	$\angle O_4HzO_1$	173.8	167.6
$\angle O_5H_4O_6$	166.8	$\angle HzO_1Al$	114.4	112.8
HzO_1AlO_2	7.6	HzO_1AlO_2	26.9	26.7
$O_4O_1AlO_2$	1.0	$H_3O_3Si_1O_2$	−32.6	−29.3
$H_1O_2AlO_1$	6.2	$O_4O_1AlO_2$	30.1	30.3
$H_2O_4O_2Al$	−120.6	$O_5O_3Si_1O_2$	−30.8	−29.6
$O_5O_4O_2Al$	−133.3	$O_5O_4O_1O_2$	−18.2	−21.39
$O_5O_4O_2O_3$	44.8	$H_1O_4O_1Al$	−36.4	−37.3
$H_3O_5O_4O_2$	−28.0	$H_2O_4O_1Al$	83.0	78.9
$H_4O_5O_4O_2$	−129.0	$H_4O_5O_3Si_1$	−123.2	−121.0
ads energy (E_{ad})				
6-31G(d,p)	−16.09		−15.79	−15.75
6-311+G(3df,2p)//	−14.57		−15.13	−14.73

be compared to our results for either H-ZSM-5 or H-FAU, and thus we defer such detailed comparisons on the energetics to the discussion section below. We only make comparisons on the adsorption structures where appropriate.

It is interesting to note that the preferred adsorption structures are quite different from both the cluster and embedded models. The optimized structure of the adsorbed neutral water dimer complex with use of the cluster model is shown in Figure 4. In this structure, one water molecule binds strongly to the $(-O)_3$-

TABLE 2: Selected Optimized Geometrical Parameters (bond lengths in Å and angles in deg) and Calculated Adsorption Energy (kcal/mol per water molecule) for Adsorption of Water Dimer on Faujasite, Using Both the Cluster and Embedded Cluster Models

cluster model		embedded cluster		
	IP (Figure 7)		NC (Figure 8)	IP (Figure 9)
O_1- - -Hz	1.32	O_1−Hz	1.10	1.38
O_2- - -H_1	1.81	O_3- - -H_3	2.13	1.91
O_3−Hz	1.11	O_4- - -Hz	1.41	1.07
O_3−H_1	1.00	O_5- - -H_1	1.58	1.45
O_3−H_2	1.00	O_1−Al	1.84	1.85
O_4- - -H_2	1.67	O_2−Al	1.73	1.79
O_4−H_3	0.97	O_2−Si_2	1.60	1.56
O_5- - -H_3	2.16	∠O_1AlO_2	98.8	94.6
O_1−Al	1.81	∠AlO_2Si_2	130.2	128.0
O_2−Al	1.77	∠$O_2Si_2O_3$	101.2	103.6
∠O_1AlO_2	98.3	∠$Si_2O_3H_3$	106.1	103.2
∠AlO_2H_1	108.3	∠$O_3H_3O_5$	169.3	166.4
∠$O_2H_1O_3$	137.5	∠$H_3O_5H_1$	109.1	116.8
∠H_1O_3Hz	99.0	∠$O_5H_1O_4$	177.7	175.7
∠O_3HzO_1	165.5	∠H_1O_4Hz	114.9	110.7
∠$O_3H_2O_4$	164.4	∠O_4HzO_1	177.2	173.9
∠$H_2O_4H_3$	116.2	∠HzO_1Al	117.5	108.8
∠$O_4H_3O_5$	162.9	HzO_1AlO_2	−2.0	−39.2
HzO_1AlO_2	18.4	$O_4O_1Al\ O_2$	−1.7	−39.6
$H_2O_2AlO_1$	−2.4	$H_1O_4O_1Al$	−9.8	66.5
$O_3O_1AlO_2$	16.1	$H_2O_4O_1Al$	−131.3	−50.0
$H_2O_3O_1Al$	−138.8	$H_3O_3Si_2O_2$	18.1	14.3
$O_1O_3O_4O_5$	−38.6	$H_4O_5O_3Si_2$	−173.0	−161.7
$O_1O_3O_4H_3$	−49.7	$O_5O_4O_1Al$	−11.2	64.2
$H_4O_4O_3O_1$	73.9	$O_5O_3Si_2O_2$	18.0	19.0
ads energy (E_{ad})				
6-31G(d,p)	−11.35		−13.82	−17.65
6-311+G(3df,2p)//	−8.46		−11.64	−14.63

Al-O(H) tetrahedral unit by forming two hydrogen bonds H1- - -O2 and Hz- - -O4 with the bond distances of 1.80 and 1.37 Å, respectively, while the other binds to the first water with the hydrogen bond distance of 1.86 Å, and has some attractions from its hydrogen atom with the zeolite framework oxygen atoms O3 and O6 with distances larger than 2.10 Å. A similar NC structure was found by Krossner and Sauer with the corresponding hydrogen bonds (similar to H1- - -O2 and Hz- - -O4) of the first water to be 1.92 and 1.37 Å, respectively. However, using a 3T cluster, Zygmunt et al.[32] found this adsorption configuration protonated, but when they repeated the study using a larger cluster model, a different adsorption structure was obtained, as discussed below. This above-mentioned structure indicates that the adsorbed complex is formed by the stepwise adsorption process. With the 7T cluster model, we were not able to find the structure corresponding to the other concerted adsorption pathway. However, using the same 5T cluster model, Zygmunt et al.[17] and Krossner and Sauer[21] found adsorption structures that corresponded to the concerted pathway where both water molecules bind to the zeolite framework to form a large ring configuration. However, their 5T cluster model consists of four H_3SiO groups tetrahedrally coordinated to the centered Al atom, thus water molecules are restricted to form hydrogen bonds with only four O atoms surrounding the Al atom. Both studies found the IP complex exists for adsorption of water dimer. The results obtained by Zygmunt et al.[17] show the NC is 2.91 more stable than IP. Using the same 5T cluster but with OH termination groups, Rice et al.[19] found only the NC complex, although having a different adsorption structure where the two water molecules also form a single large ring with the zeolite framework, but one is hydrogen bonded to the OH termination group. Such hydrogen bonding does not exist in the 5T model used by Zygmunt et al.[17] and Krossner and Sauer.[21] The differences in these results indicate that the 5T cluster model is not sufficient due to large boundary effects. The 7T cluster model used in this study attempted to remove much of these effects so that there is no restriction on the hydrogen-bond configuration of water dimer with the Brønsted acid site and zeolite framework.

When the Madulung potential is included, both NC (Figure 5) and IP (Figure 6) are observed with similar structures where the two water molecules form a single large 7-membered ring-like structure (counting only heavy atoms) with the zeolite framework. There are three hydrogen bonds in this adsorption configuration in which the two water molecules form a hydrogen bond between each other and each water molecule forms one hydrogen bond with the zeolite framework. This adsorption configuration supports the concerted adsorption pathway as seen in previous studies by Zygmunt et al.,[17] Krossner and Sauer,[21] and Rice et al.[19]

Taking a closer look at the NC and IP adsorption structures from the embedded cluster calculations as shown in Figures 5 and 6, respectively, we found that these structures are quite similar to the NC structure obtained by Rice et al. For the NC complex, the first hydrogen bond arises from the interaction of the oxygen atom of one of the two water molecules and the acidic proton (O4- - -Hz), which is calculated to be 1.27 Å. This value is comparable with 1.26 Å from Rice et al.'s structure but is noticeably shorter than the value of 1.49 Å determined by Zygmunt et al. The second hydrogen bond is formed between two water molecules, which are considered as the adsorbate−adsorbate interaction, with the distance of 1.49 Å. This is slightly shorter than the value of 1.55 Å from Rice et al., but is also significantly shorter than the value of 1.70 Å from Zygmunt et al. The third hydrogen bond is from the hydrogen atom of the other water molecule, H3, and the oxygen O3 of the zeolite framework with the distance of 1.83 Å. This value is slightly longer than the value of 1.72 Å from Rice et al.'s structure and is comparable with 1.78 Å from Zygmunt et al.'s structure. However, as mentioned earlier in Zygmunt et al.'s structure, the two water molecules are restricted to form hydrogen bonds with four oxygen atoms bonded to the Al atom only (see Figure 1 in ref 17).

The IP adsorption complex has a similar overall structure with the NC complex, except that the Brønsted proton is transferred to the water (specifically to the O4 atom in Figure 6). Consequently, it changes the hydrogen bond pattern and distances. Particularly, the first hydrogen bond arises from the interaction of the oxygen atom O1 of ZSM-5 and the acidic proton (O1- - -Hz), which is calculated to be 1.49 Å. This value is more or less the same as the IP determined by Zygmunt et al. The water−water hydrogen bond (O5- - -H1) distance of 1.22 Å is significantly shorter than any previously calculated values, which are above 1.50 Å. The remaining hydrogen bond between the H3 hydrogen atom in the second water and the O3 atom of zeolite framework is calculated to be 1.65 Å. This is in the range from 1.50 to 1.78 Å of previously reported values. It is interesting to note that the protonated $H_5O_2^+$ ion has the angle O4H1O5 of 177.4°, the H1O5 and H1O4 distances of 1.22 and 1.18 Å, respectively, and the relative orientation of the two water molecules (see Figure 6). This configuration is closer to the configuration of $H_5O_2^+$ ion, where the proton is equally shared between the two water molecules, than the H_3O^+- - -H_2O configuration.

A number of experiments have been done with the FTIR technique to characterize and distinguish the IP water−zeolite

TABLE 3: Comparisons of Calculated Adsorption Energies of $(H_2O)_2$/Zeolite with Previous Theoretical and Experimental Results

level of theory	cluster	model	mode	ΔE	ref
H-ZSM-5					
B3LYP/'big'//	7T	cluster	NC	−14.57	*b*
B3LYP/'big'//	7T	embedded	NC	−15.13	*b*
B3LYP/'big'//	7T	embedded	IP	−14.73	*b*
B3LYP/6-31G(d,p)	5T	cluster	NC	−11.8	23
BP/DZP (H, Si, Al) TZP (O)	5T (generic)	cluster	IP	−14.28	24
B3LYP/6-31+G(d,p)	5T	cluster	NC-IP	(2.31)[a]	25
experiment				−8.2	26
Faujasite					
B3LYP/'big'//	7T	cluster	NC	−11.64	*b*
B3LYP/'big'//	7T	cluster	IP	−8.46	*b*
B3LYP/'big'//	7T	embedded	IP	−14.63	*b*
BP/DZP (H, Si, Al) TZP (O)	5T (generic)	cluster	IP	−14.28	24

[a] Relative energy. [b] This work.

complexes from the neutral ones.[4,13,14,33] However, interpretation of IR spectra of water in zeolites with different loading levels has been rather difficult and not without ambiguity. The reason can be best illustrated by Zecchina et al.'s remark "all the arguments developed so far for the basic IR spectroscopy of the (OH- - -B) groups also hold for the (O^-- - -$^+$HB) species and that a clear cut between the two cases is not straightforward".[14] For adsorption of a single water molecule (corresponding to 10^{-5}−10^{-4} mbar of vapor pressure), both experimental and theoretical studies strongly support the neutral species. Even so, there are features on their IR spectra, such as the broad continuum band covering the 3000 to 1300 cm^{-1} range and the strong peak in the region of 1860−1650 cm^{-1}, that cannot be explained by existing arguments. For higher loading levels, i.e., $(H_2O)_n$ in H-ZSM-5 zeolite with $n > 1$, although the interpretation of the experimental IR spectra is even more difficult, there has been some consensus that dimeric $H_5O_2^+$ species were observed, thus our present results are consistent with the previous IR results. In this study, we have further calculated the IR spectra for the IP and neutral water dimer complexes in H-ZSM-5 using the embedded cluster model, then compared the results with the experimental spectra.

FTIR spectra for water in H-ZSM-5 under an equilibrium pressure between 10^{-3} to 10^{-2} mbar done by Jentys et al.[4] show a strong increase in the four bands at 3695, 2885, 2457, and 1630 cm^{-1}. The authors suggested that these four bands are characteristics of the hydroxonium $H_5O_2^+$ species adsorbed on the negative charge ZSM-5 zeolite framework. In particular, the band at 3695 cm^{-1} is due to the free OH group pointing away from the zeolite framework; the two broad bands at 2885 and 2457 cm^{-1} are of the O- - -H^+- - -O part; and the band around 1630 cm^{-1} is due to deformation of the H_3O^+ component. Zecchina et al.,[14] on the other hand, suggested the two main fingerprints for hydroxonium $H^+(H_2O)_n$ species on IR spectra of water in H-ZSM-5 zeolite are an adsorption in the 1860−1650 cm^{-1} range, accompanied by a partner around 1455 cm^{-1}, in addition to the broad "continuum" band from 1300 to 3000 cm^{-1} due to different $H^+(H_2O)_n$ species pointed out in their earlier study.[33] However, experimental spectra alone cannot precisely determine the number of H_2O molecules solvating the acidic proton. Kondo et al. later added another feature for the dimeric $H_5O_2^+$ species that is the band at 3207 cm^{-1}.

The main features of our calculated IR spectra for water dimer adsorption in H-ZSM-5 zeolite for both the NC and IP complexes are listed in Table 4. The calculated frequencies were not scaled. The characteristic vibrational modes of the bridged

TABLE 4: Calculated Unscaled Vibrational Frequencies ν (cm^{-1}) and Intensities I (KM/mol) for the NC and IP Complexes on H-ZSM-5

neutral complex		ion-pair complex	
mode	ν and (I)	mode	ν and (I)
ν(O 4H2)	3864 (54)	ν(O4H2)	3849 (89)
ν(H 3O5H4) asym	3845 (776)	ν(O5H4)	3824 (151)
ν(O5H4)	3841 (1862)	ν(O5H3)	3179 (948)
ν(O5H3)	3552 (665)	(H1O4Hz) sym	2507 (1488)
ν(OHz) + ν(O4H1)	2726 (1571)	$\delta(H_3O^+)$	1675 (417)
δ(H1O4H2)	1722 (251)	$\delta(H_3O^+)$	1760 (92)
δ(H3O5H4)	1669 (41)	δ(H3O5H4)	1707 (224)
δ (OHz)	1521 (87)	$\delta(H_3O^+)$ umb	1350 (420)
γ(OHz)	1472 (690)		
ν(OHz)	1313 (773)		

hydroxyl group are assigned as in Figure 10. We first discuss features of the $H_5O_2^+$ IP complex. The calculated vibrational frequencies at 3849 cm^{-1} correspond to the ν(OH) of the free OH bond of the adsorbed $H_5O_2^+$ (see Figure 6), with the O4H2 is pointing away from the zeolite framework, which is in reasonable agreement with experimental observation[4] at 3700 cm^{-1}. The peaks at 3824 and 3179 cm^{-1} are of the second H_2O moiety, which are close to the calculated frequency results of 3884 and 3275 cm^{-1} obtained by Zygmunt et al.[17] The former is assigned to the ν(O5H4) of the free OH group, The latter belongs to the ν(O5H3), the frequencies shift due to one hydrogen atom being bonded to the zeolite framework (H3). The latter peak is in good agreement with the fingerprint at 3207 cm^{-1} suggested by Kondo et al.[13] The calculated peaks at 1760 and 1675 cm^{-1} are assigned to be the bending mode of the hydroxonium species, $\delta(H_3O^+)$, which is comparable to the frequency range of 1860−1650 cm^{-1}, the fingerprints of protonated $H^+(H_2O)_n$ species obtained by Zecchina et al.,[14] and are also consistent with the experimental observation band at 1630 cm^{-1} by Jentys et al.[4] The frequency at 2507 cm^{-1} belongs to symmetric stretch modes, ν(HzO4H1), of the two hydrogen bonds of the hydroxonium ion, O4Hz and O4H1, respectively (see Figure 6), which is comparable to the peak of symmetric $\nu(H_3O^+)$ at 2911 cm^{-1} from Zygmunt et al. The 1350 cm^{-1} corresponds to the umbrella mode, the characteristic of the protonated water clusters, as pointed out by Zecchina et al.

For the neutral water dimer complex, we found that the peak at 2726 cm^{-1} belongs to the OH stretching mode of the acidic site, ν(O1Hz), being very intense because it overtones with the ν(O4H1) mode (see Figure 5). This is in good agreement with the experimental result of the ν(OH- - -O) mode of group a at 2680 cm^{-1} for a neutral complex of a single water adsorption on H-ZSM-5 (see Scheme 6 in ref 14). The peak at 1472 cm^{-1} assigned to the γ(OH- - -O) mode is in agreement with the frequency peak at 1415 cm^{-1} from Zygmunt et al. The peak at 1521 cm^{-1} is the δ(O1Hz), the bending mode of the acidic OH group. The peaks at 1722 and 1669 cm^{-1} belong to δ(HOH), the bending mode of the first water and the second water, respectively. The lower frequency peak is comparable to the peak at 1684 cm^{-1} calculated by Zygmunt et al. Unfortunately, we cannot make a direct comparison between our calculated IR spectrums for the NC of water dimer adsorption on H-ZSM-5 with that of Zecchina et al. since the latter was interpreted for a single water molecule adsorption. Our result for the structure of the neutral dimer complex is quite different from those known for the neutral monomer complex.[17,21]

Since our results suggested both the neutral and IP complexes can exist in equilibrium in H-ZSM-5, we merge the IR features of both complexes so as to predict fingerprints for these species. Results from Table 4 confirmed the difficulty in interpreting

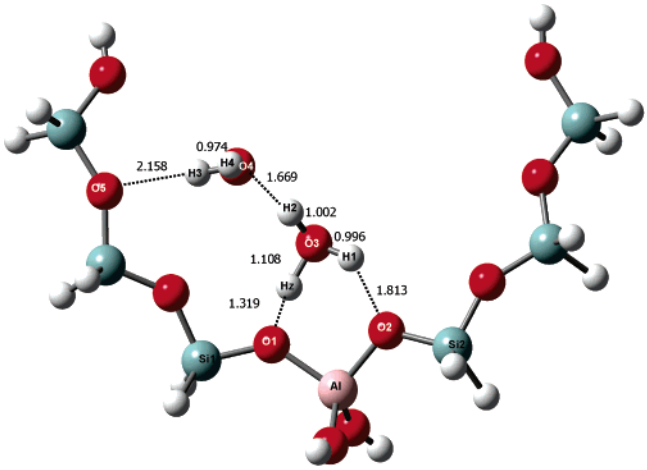

Figure 7. Structure of the ion-pair complex of the $(H_2O)_2$/H-Faujasite system optimized at the B3LYP/6-31G(d,p) level, using the cluster model (bond distances are in Å).

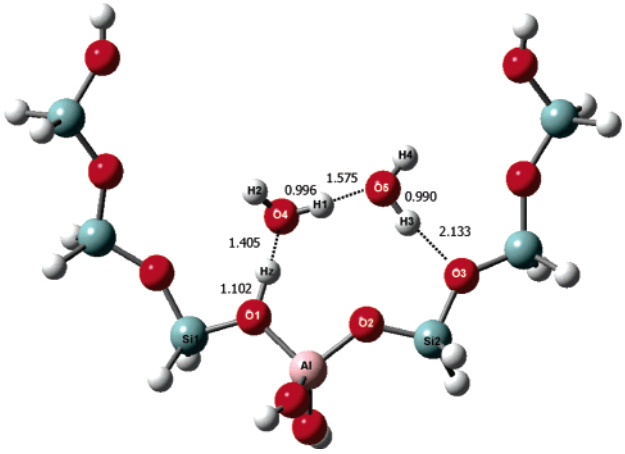

Figure 8. Structure of the neutral complex of the $(H_2O)_2$/H-Faujasite system optimized at the B3LYP/6-31G(d,p) level, using the cluster model (bond distances are in Å).

experimental IR spectra. Most bands for the water dimer in the neutral and IP complex forms overlap with consideration of broadening due to different possible configurations of these species. There is one band peaking at 3179 cm^{-1} in the IP complex that appeared to be the most distinct fingerprint for the dimeric $H_5O_2^+$ species, and this is in excellent agreement with that suggested by Kondo et al. By examining the relative intensities, our results also support the adsorption in the region 1865−1650 cm^{-1} suggested by Zecchina et al. and Jentys et al. as another fingerprint for the protonated $H^+(H_2O)_n$ species.

Adsorption of Water Dimer on H-FAU. Optimized adsorption structures of water dimer on H-FAU are shown in Figures 7 and 8 using the cluster model, and Figure 9 using the embedded cluster model. Selected bond distances are also given in these figures. Additional selected optimized geometrical parameters and calculated adsorption energies are listed in Tables 2 and 3, respectively. The cluster model predicts that both the NC and IP complexes exist with the NC being more stable with the ZPE corrected adsorption energy of −11.64 kcal/mol as compared to that of −8.46 kcal/mol for the IP complex. However, when the Madelung field is included, only the IP complex was found with the ZPE-corrected adsorption energy of −14.63 kcal/mol. This is very different when compared to the results for adsorption of water dimer on H-ZSM5 zeolite, where the cluster model predicts only the NC complex, while the embedded cluster model yields both the NC and IP

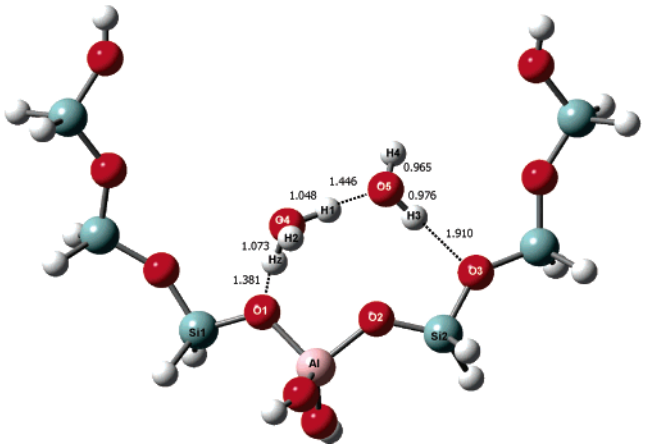

Figure 9. Structure of the ion-pair complex of the $(H_2O)_2$/H-Faujasite system optimized at the B3LYP/6-31G(d,p) level, using the embedded cluster model (bond distances are in Å).

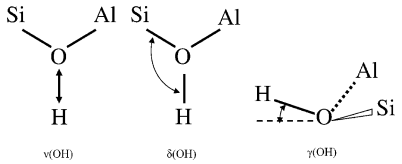

Figure 10. The characteristic vibrational modes of the bridged hydroxyl group.

complexes. It is interesting to note that although the cluster models for both H-ZSM-5 and H-FAU have the same 7T sites, they were cut out from the actual cross section of the crystal structures of these zeolites, thus they have different 3D structures. Therefore, we observed different results for adsorption on H-ZSM-5 and H-FAU zeolites, even using only the cluster model. Previous studies[17,21] used generic cluster models to represent the Brønsted acidic site and thus did not include any effects of the crystal framework. Similar to the adsorption on H-ZSM5, both the cluster and embedded cluster models predict different results on the adsorption structures.

Optimized adsorption structures for the IP and NC complexes with the 7T cluster model are shown in Figures 7 and 8, respectively. Since we have already provided more detailed comparisons between the adsorption structures of water dimer on H-ZSM-5 with results from previous generic cluster models in the previous subsection, it is more informative here to also provide some discussion on the differences on adsorption structures of water dimer on H-ZSM-5 and H-FAU zeolites.

The IP adsorption structure from the cluster model (Figure 7) has the protonated form: the water molecule binds strongly to the two oxygen atoms of the $(-O)_3$-Al-OH tetrahedral unit while the other water binds weakly to the zeolite framework. This structure supports the stepwise adsorption pathway. In particular, this complex has a total of four hydrogen bonds. The first two hydrogen bonds arise from interactions of the two Hz and H1 of the protonated water with O1 and O2 atoms of the acidic site with bond distances of 1.32 and 1.81 Å, respectively. The other H of H_3O^+, namely H2, bonds to the O4 atom of the second water with the bond length of 1.67 Å. Finally, the fourth hydrogen bond is between the H3 atom of the second water and the O5 atom of extended zeolite. This structure is similar to the NC complex in H-ZSM-5 using the cluster model, except in this case the water dimer is protonated. The more stable NC complex from the cluster model, on the other hand, has the water dimer forming two hydrogen bonds with the acidic site in a single 7-member ring-like structure as mentioned earlier for the

TABLE 5: Comparisons between Calculated Unscaled Vibrational Frequencies ν (cm^{-1}) and Intensities I (KM/mol) of the Ion-Pair Complexes in H-Faujasite and H-ZSM-5

ion-pair on Fau		ion-pair on ZSM-5	
mode	ν and (I)	mode	ν and (I)
ν(O 4H2)	3782 (135)	ν(O4H2)	3849 (89)
ν(H3O5H4) sym	3662 (375)	ν(O5H4)	3824 (151)
ν(H3O5H4) asym	3889 (139)	ν(O5H3)	3179 (948)
ν(HzO4H1) sym	2516 (1598)	(H1O4Hz) sym	2507 (1488)
ν(HzO4H1) asym	2025 (3389)	$\delta(H_3O^+)$	1675 (417)
δ(H3O5H4) + $\delta(H_3O^+)$	1627 (48)	$\delta(H_3O^+)$	1760 (92)
$\delta(H_3O^+)$	2726 (1571)	δ(H3O5H4)	1707 (224)
$\delta(H_3O^+)$ umb	1391 (480)	$\delta(H_3O^+)$ umb	1350 (420)

concerted adsorption pathway. One hydrogen bond is between the Brønsted proton and the O4 atom of one of the two water molecules with the distance of 1.41 Å and the other is between the H3 atom of the other water molecule with the O3 atom of the zeolite framework with the distance of 2.13 Å. The hydrogen bond between the two water molecules has the distance of 1.58 Å. This structure is quite similar to that observed for adsorption on H-ZSM-5 with the embedded cluster model (Figure 5), except that all hydrogen bonds in this case are noticeably longer by 0.09 to 0.18 Å.

When the effect of lattice framework is taken into account, only the protonated species (Figure 9) is observed with the ZPE-corrected adsorption energy of −14.63 kcal/mol. The structure is similar to those from the concerted adsorption pathway that has three hydrogen bonds stabilizing the ionic species. The two hydrogen bonds between the hydrogen atoms of the $H_5O_2^+$ species and the oxygen atoms of the zeolite framework, namely the Hz- - -O1 and H3- - -O3, have bond distances of 1.38 and 1.91 Å, respectively. The hydrogen bond between the two water molecules, H1- - -O5, has the distance of 1.45 Å. On closer look at the structure of the protonated $H_5O_2^+$ species, we find that in addition to the H1- - -O5 distance of 1.45 Å, the O4H1, O4Hz, and O4H2 bond distances of 1.05, 1.07, and 1.00 Å, respectively, and the angle O4H1O5 of 175.7° indicate the protonated $H_5O_2^+$ has the configuration of H_3O^+- - -H_2O. This is very different from that observed for the adsorption of water dimer on H-ZSM-5 zeolites (Figure 6), which has the configuration of H_2O- - -H^+- - -OH_2, where the proton is shared between two water molecules. A possible explanation for such differences is given below in the discussion section.

Since the experimental IR spectrum is not available for water adsorption in H-Faujasite, in this subsection we present our calculated IR spectra for the $H_5O_2^+$ IP complex using the embedded cluster model and compare the results with those for the water in the H-ZSM-5 zeolite system. Calculated observable bands due to the water dimer component in the IP complex for adsorption in both H-FAU and H-ZSM-5 are listed in Table 5. Similarly, the calculated frequencies were not scaled. The frequency of 3782 cm^{-1} corresponds to the ν(O4H2) stretch mode of the free OH group, which is lower than the 3849 cm^{-1} frequency of H-ZSM-5 (see Figure 9). This is due to the free O4H2 bond distance for the protonated species in H-FAU being slightly longer.

The second water in H_3O^+- - -H_2O in H-FAU can be considered as an outer water layer, which is quite different compared to that of the H_2O- - -H^+- - -OH_2 complex in H-ZSM-5 where it shares the proton with the other water molecule. Therefore, we were able to observe the clear H_2O moiety in the H-FAU channel: two OH stretching frequencies in the 3200−3900 cm^{-1}, one at 3889 cm^{-1} belonging to the anti-symmetric OH stretch, ν(H4O5H3), and the peak at 3662 cm^{-1} corresponding to the symmetric OH stretching mode, whereas in H-ZSM-5 we obtain two separated OH stretching modes of the second water, namely ν(O5H4) and ν(O5H3). It is interesting to note that we found there are both the symmetric and anti-symmetric OH stretching modes involving the two hydrogen-bonded hydrogen atoms of the H_3O^+ moiety, ν(HzO4H1), that have a relatively high intensity at 2516 and 2025 cm^{-1}, while in H-ZSM-5 only the symmetric stretching mode, ν(HzO4H1), at 2507 cm^{-1}, was observed. In addition, the umbrella mode, which is a characteristic of the H_3O^+ moiety, at 1391 cm^{-1} is in a higher region and more intense than that of 1350 cm^{-1} in H-ZSM-5 due to the protonated species in H-FAU having more characteristics of H_3O^+ than that of H-ZSM-5.

Discussion

In our present study for adsorption of water dimer, we found that both the neutral and ion-pair complexes can coexist in H-ZSM-5 and only ion-pair complex is predicted in H-FAU zeolites. Furthermore, we also found that these adsorption complexes can be formed from two different pathways, namely the stepwise and concerted adsorption pathways. The cluster model predicts adsorption of water dimer on H-ZSM-5 resulting only in the neutral complex. However, including the effects of the zeolite lattice framework by using the embedded cluster model, we found that the ion-pair complexes are stable in both the H-ZSM-5 and H-Faujasite systems from only the concerted adsorption pathway. This indicates that the Madelung potential has the effect of stabilizing the protonated species. However, these protonated species have significantly different configurations. The IP for water dimer in H-ZSM-5 has the H_2O- - -H^+- - -H_2O configuration where the proton is shared between the two water molecules, whereas the IP for water dimer in H-FAU has the H_3O^+- - -H_2O configuration where the proton is associated with only one particular water molecule. This is due to the fact that ZSM-5 has the smaller 10-membered ring pore size of 5.6 Å as compared to the 12-membered ring pore size of 7.4 Å in FAU. To understand how the pore size affects the adsorption structure of water dimer, let us examine the potential surface of the isolated $H_5O_2^+$ system.[34−37] The isolated $H_5O_2^+$ system has a double-well potential energy surface (PES) with the H_3O^+- - -H_2O configuration where the proton is associated with one or the other water molecules and is a stable equilibrium structure while the H_2O- - -H^+- - -OH_2 configuration where the proton is equally shared between the two water molecules is the transition state for proton transfer between these two stable configurations. As the O−O distance decreases, the double-well PES is transformed into a single-well where the transition state configuration becomes the stable equilibrium structure. Since the ZSM-5 zeolite has a noticeably smaller pore size than that of FAU, it forces the two water molecules closer together as indicated by the O−O distance of 2.40 Å in the IP complex as compared to that of the 2.49 Å in the IP complex FAU. Since the barrier for proton transfer in the dimer $H_5O_2^+$ complex is only about 0.6 kcal/mol,[17] the decrease in the O−O bond distance by 0.09 Å can lead to the PES of the $H_5O_2^+$ moiety becoming a single-well, and thus the H_2O- - -H^+- - -H_2O configuration is stabilized in ZSM-5 rather than a double-well as in the FAU. These results show that the spatial confinement effects are rather important in understanding adsorption properties in zeolite.

The predicted adsorption energy of ion-pair complexes at the B3LYP/6-311+G(3df,2p) level of theory with inclusion of the zero-point energy corrections is −14.73 kcal/mol for H-ZSM-5 and −14.63 kcal/mol for H-Faujasite, which are considered as

more or less the same adsorption energies. The neutral water dimer complex only exists in the H-ZSM-5 zeolite with the adsorption energy of −15.13 kcal/mol. This can be compared to the experimental adsorption energy of 8.2 kcal/mol per two water molecules per cation obtained by Gorte et al.,[2] which was derived by measuring the equilibrium infrared spectra as a function of vapor pressure and temperature. Since it has been known that H-ZSM-5 is more acidic than H-FAU, one would expect that protonation of water dimer is easier and adsorption energy of water dimer in H-ZSM-5 would also be larger as compared to those of the H-FAU zeolite. Our results indicate that the adsorption properties depend not only on the acid strength of zeolites but also on the topologies of those zeolites. Note that in comparison with previous theoretical studies as listed in Table 3, Zygmunt et al. found that the neutral complex is more stable compared to the protonated dimer complex by 2.9 kcal/mol while the barrier for the deprotonation step (the reverse direction) is very small. Krossner and Sauer found that both NC and IP structures are minima on the potential energy surface; the NC complex is less stable compared to the IP complex by 3.6 kcal/mol. These two results are conflicting in order of stabilities. Our results indicate that, particularly for the H-ZSM-5 zeolite, both NC and IP are present as local energy minima on the potential energy surface with a small energy difference of 0.40 kcal/mol, thus they can be in thermal equilibrium and almost equal in population.

Comparisons between calculated IR spectra of the NC and IP complexes on H-ZSM-5 zeolites suggest several distinct bands for the protonated species which are consistent with experimental interpretations, namely the free OH stretch band at 3179 cm^{-1} and the band corresponding to the bending mode of hydroxonium in the region 1675−1760 cm^{-1}. These bands do not exist for the protonated H_3O^+- - -H_2O species in H-FAU due to the differences in the adsorption structure. It should be noted that in the actual experimental condition of a given vapor pressure, there can be a wide range of adsorbed water clusters of different sizes existing. Even for clusters of the same size, they can be very different in their structures due to their relative orientations in the zeolite framework. For this reason, the experimental IR spectra tend to have broad bands and are difficult to interpret. Our calculations here provide molecular-level insights into the interpretations of these spectra.

Conclusion

We have performed a systematic theoretical study on the modes of adsorption of water dimer on H-ZSM-5 and H-FAU zeolites using an embedded cluster approach with the hybrid B3LYP density functional method. Our results indicate that there are two possible adsorption pathways: a stepwise and a concerted adsorption process. The stepwise process involves adsorption of one water at a time and results in a complex where the first water binds more strongly to the $(-O)_3$-Al-OH tetrahedral unit making a 6-membered ring structure similar to that of the adsorption of a single water molecule and the second water molecule does not have any direct interaction with the adsorption site but binds to the other water and the zeolite framework. The concerted adsorption pathway yields the adsorption structure that has both water molecules binding to the adsorption site forming a single larger ring where one of the two water molecules makes only one hydrogen bond to the Brønsted site and the other water forms a hydrogen bond with the oxygen atom of the nearby tetrahedral unit. We found that for adsorption on H-ZSM-5 zeolite, both the neutral and ion-pair complexes can exist with adsorption energies of −15.13 and −14.73 kcal/mol, respectively. The relatively small difference in the adsorption energy indicates that both forms of complexes can exist in experimental conditions that are almost equal in population. For adsorption on the H-Faujasite, only the ion-pair complex exists with the adsorption energy of −14.63 kcal/mol. Our results indicate that adsorption properties depend not only on the acidity of the Brønsted acidic site but also on the topology of the zeolite framework, such as on the spatial confinement effects noted in this study. Such spatial confinement effects have led to different structures for the ion-pair complexes on H-ZSM-5 and H-FAU zeolites despite their adsorption energies being quite similar. In particular, the smaller channel cross section of the H-ZSM-5 zeolite results in the $H_5O_2^+$ species having the proton almost equally shared between the two water molecules that resembles the transition state configuration H_2O- - -H^+- - -H_2O on the isolated $H_5O_2^+$ potential energy surface, whereas the larger channel cross section H-FAU yields the ion-pair complex, where the proton is associated with one particular water molecule, i.e., H_3O^+- - -H_2O. The differences in these ion-pair complexes have led to distinct differences in their IR spectra. Our calculated IR spectra confirm several fingerprints for the ion-pair complexes on zeolites as suggested in previous experimental IR studies.

Acknowledgment. This work was supported in part by grants from the Thailand Research Fund (TRF Senior Research Scholar to J.L.), the Kasetsart University Research and Development Institute (KURDI), the Ministry of University Affairs under the Science and Technology Higher Education Development Project (MUA-ADB funds), as well as the ACS PRF grant to T.N.T.. The support from the Dow Chemical Company (U.S.A.) and the computer resources provided by the University of Utah Center for High Performance Computing are also acknowledged.

References and Notes

(1) Greatbanks, S. P.; Hillier, I. H.; Burton, N. A.; Sherwood, P. *J. Chem. Phys.* **1996**, *105*, 3770.
(2) Ison, A.; Gorte, R. J. *J. Catal.* **1984**, *89*, 150.
(3) Mirth, G.; Lercher, J. A.; Anderson, M. W.; Klinowski, J. *J. Chem. Soc., Faraday Trans.* **1990**, *86*, 3039.
(4) Jentys, A.; Warecka, G.; Derewinski, M.; Lercher, J. A. *J. Phys. Chem.* **1989**, *93*, 4837.
(5) Haase, F.; Sauer, J. *J. Am. Chem. Soc.* **1995**, *117*, 3780.
(6) Bates, S.; Dwyer, J. *THEOCHEM* **1994**, *112*, 57.
(7) Pelmenschikov, A. G.; van Santen, R. A. *J. Phys. Chem.* **1993**, *97*, 10678.
(8) Marchese, L.; Chen, J.; Wright, P. A.; Thomas, J. M. *J. Phys. Chem.* **1993**, *97*, 8109.
(9) Limtrakul, J. *Chem. Phys.* **1995**, *193*, 79.
(10) Nusterer, E.; Bloechl, P. E.; Schwarz, K. *Angew. Chem., Int. Ed. Engl.* **1996**, *35*, 175.
(11) Kogelbauer, A.; Nikolopoulos, A. A.; Goodwin, J. G.; Marcelin, G. *J. Catal.* **1995**, *152*, 122.
(12) Limtrakul, J.; Treesukol, P.; Ebner, C.; Sansone, R.; Probst, M. *Chem. Phys.* **1997**, *215*, 77.
(13) Kondo, J. N.; Iizuka, M.; Domen, K.; Wakabayashi, F. *Langmuir* **1997**, *13*, 747.
(14) Zecchina, A.; Geobaldo, F.; Spoto, G.; Bordiga, S.; Ricchiardi, G.; Buzzoni, R.; Petrini, G. *J. Phys. Chem.* **1996**, *100*, 16584.
(15) Jobic, H.; Tuel, A.; Krossner, M.; Sauer, J. *J. Phys. Chem.* **1996**, *100*, 19545.
(16) Termath, V.; Haase, F.; Sauer, J.; Hutter, J.; Parrinello, M. *J. Am. Chem. Soc.* **1998**, *120*, 8512.
(17) Zygmunt, S. A.; Curtiss, L. A.; Iton, L. E. *J. Phys. Chem. B* **2001**, *105*, 3034.
(18) Gale, J. D. *Top. Catal.* **1996**, *3*, 169.
(19) Rice, M. J.; Chakraborty, A. K.; Bell, A. T. *J. Phys. Chem. A* **1998**, *102*, 7498.
(20) Limtrakul, J.; Nokbin, S.; Chuichay, P.; Khongpracha, P.; Jungsuttiwong, S.; Truong, T. N. *Stud. Surf. Sci. Catal.* **2001**, *135*, 2469.
(21) Krossner, M.; Sauer, J. *J. Phys. Chem.* **1996**, *100*, 6199.

(22) Zygmunt, S. A.; Curtiss, L. A.; Iton, L. E.; Erhardt, M. K. *J. Phys. Chem.* **1996**, *100*, 6663.

(23) Zygmunt, S. A.; Curtiss, L. A.; Zapol, P.; Iton, L. E. *J. Phys. Chem. B* **2000**, *104*, 1944.

(24) Mortier, W. J.; Van den Bossche, E.; Uytterhoeven, J. B. *Zeolites* **1984**, *4*, 41.

(25) Alvarado-Swaisgood, A. E.; Barr, M. K.; Hay, P. J.; Redondo, A. *J. Phys. Chem.* **1991**, *95*, 10031.

(26) Derouane, E. G.; Fripiat, J. G. *Zeolites* **1985**, *5*, 165.

(27) Treesukol, P.; Limtrakul, J.; Truong, T. N. *J. Phys. Chem. B* **2001**, *105*, 2421.

(28) Stefanovich, E. V.; Truong, T. N. *J. Phys. Chem. B* **1998**, *102*, 3018.

(29) Limtrakul, J.; Jungsuttiwong, S.; Khongpracha, P. *J. Mol. Struct.* **2000**, *525*, 153.

(30) Limtrakul, J.; Khongpracha, P.; Jungsuttiwong, S.; Truong, T. N. *J. Mol. Catal. A* **2000**, *153*, 155.

(31) Frisch, M. J.; Trucks, G. W.; Schlegel, H. B.; Scuseria, G. E.; Robb, M. A.; Cheeseman, J. R.; Zakrzewski, V. G.; Montgomery, J. A., Jr.; Stratmann, R. E.; Burant, J. C.; Dapprich, S.; Millam, J. M.; Daniels, A. D.; Kudin, K. N.; Strain, M. C.; Farkas, O.; Tomasi, J.; Barone, V.; Cossi, M.; Cammi, R.; Mennucci, B.; Pomelli, C.; Adamo, C.; Clifford, S.; Ochterski, J.; Petersson, G. A.; Ayala, P. Y.; Cui, Q.; Morokuma, K.; Malick, D. K.; Rabuck, A. D.; Raghavachari, K.; Foresman, J. B.; Cioslowski, J.; Ortiz, J. V.; Stefanov, B. B.; Liu, G.; Liashenko, A.; Piskorz, P.; Komaromi, I.; Gomperts, R.; Martin, R. L.; Fox, D. J.; Keith, T.; Al-Laham, M. A.; Peng, C. Y.; Nanayakkara, A.; Gonzalez, C.; Challacombe, M.; Gill, P. M. W.; Johnson, B. G.; Chen, W.; Wong, M. W.; Andres, J. L.; Head-Gordon, M.; Replogle, E. S.; Pople, J. A. Gaussian 98, revision A.7; Gaussian, Inc.: Pittsburgh, PA, 1998.

(32) Zygmunt, S. A.; Curtiss, L. A.; Iton, L. E.; Erhardt, M. K. *J. Phys. Chem.* **1996**, *100*, 6663.

(33) Buzzoni, R.; Bordiga, S.; Ricchiardi, G.; Spoto, G.; Zecchina, A. *J. Phys. Chem.* **1995**, *99*, 11937.

(34) Kim, Y.-H.; Lee, I.-H.; Martin, R. M. *AIP Conf. Proc.* **2000**, *501*, 366.

(35) Lami, A.; Villani, G. *THEOCHEM* **1995**, *330*, 307.

(36) Krokidis, X.; Vuilleumier, R.; Borgis, D.; Silvi, B. *Mol. Phys.* **1999**, *96*, 265.

(37) Ojamae, L.; Shavitt, I.; Singer, S. J. *Int. J. Quantum Chem., Quantum Chem. Symp.* **1995**, *29*, 657.